Miniaturized Planar-Patch Antenna Based on Metamaterial L-shaped Unit-Cells for Broadband Portable Microwave Devices and Multiband Wireless Communication Systems

Mohammad Alibakhshikenari [1]*, Bal S. Virdee [2], Abdul Ali [1], and Ernesto Limiti [1]

[1] Electronics Engineering Department, University of Rome "Tor Vergata", Via del politecnico 00133, Rome, ITALY
[2] London Metropolitan University, Center for Communications Technology & Mathematics, School of Computing & Digital Media, London N7 8DB, UK

*alibakhshikenari@ing.uniroma2.it

Abstract: **This paper describes the design of a metamaterial planar antenna for multi-octave band operation. The metamaterial unit-cell comprises L-shaped slit which is etched inside a rectangular patch with grounded inductive spiral. The slit essentially behaves as a series left-handed capacitance and the spiral as a shunt left-handed inductance. The antenna was modeled and optimized for impedance bandwidth, gain and efficiency performance using commercial 3D full-wave electromagnetic simulation tools. The antenna has a measured impedance bandwidth of 6.02 GHz for S_{11} < -10 dB. This corresponds to a fractional bandwidth of 172.49 %, which is higher than multiband planar antennas reported to date. The antenna has a maximum gain and efficiency performance of 3.7 dBi and 73 %, respectively, at 3.25 GHz. The physical footprint of the antenna is comparable to other wideband planar antennas reported to date. The overall size of the antenna is $0.037\lambda_0 \times 0.027\lambda_0 \times 0.002\lambda_0$ and $0.25\lambda_0 \times 0.18\lambda_0 \times 0.017\lambda_0$, where λ_0 is free-space wavelength at 0.48 and 3.25 GHz, respectively.**

Keywords: **Composite right/left-handed (CRLH), metamaterial (MTM), planar antenna, tri-band antenna.**

I. INTRODUCTION

Integration of multiple communication standards in a wireless system is becoming more and more common practice in order to effectively improve the portability of wireless communications devices. This has led to a growing demand for low profile miniature antennas with multiband operation. As a result, various types of antennas have been explored [1]–[7]. Planar monopole antenna is often adopted to realize multiband operation, with various structures such as meandered T-shape [1], flared shape with V-sleeve [2], Y-shape [3], and multi-fractal structure [4]. These antennas exhibit desirable characteristics including simple structure, low profile and weight, versatile structure for wide impedance bandwidth, and regular omnidirectional radiation patterns. However, the bulky size of such antennas can restrict their applications in compact portable wireless systems. So far, for size reduction, many slot structure based antennas [5]–[7] have been proposed. In [5] and [6], antennas with multiple meandering slots are designed to generate multiple resonant modes. Combined with an L-probe feed, the use of U-slots can also yield dual-band and multiband characteristics [7]. These slot structure based antennas are much smaller than the traditional monopoles. But their structures are much more complex for practical applications. To overcome these limitations, we have implemented a novel antenna structure based on metamaterial technology with low profile, weight and simplicity in manufacturing accompanying desirable performance parameters including small electrical size, multiband performance and good radiation characteristics.

Metamaterials (MTMs) are beginning to attract significant attention in the development of antennas due to their unique electromagnetic properties, such as anti-parallel phase and group velocities and zero propagation constant [8]. MTMs have been successfully exploited to develop small resonant antennas [9]–[11]. A dual-band MTM antenna for WiFi applications was shown in [12] and multiband MTM resonant antennas were shown to exhibit several left-handed modes in [13]. Although the resonant frequency of the MTM structure depends on the makeup of the composite right/left-handed (CRLH) transmission-lines (TL) unit-cell rather than the antenna's physical size, however, metamaterial antennas suffer from narrow bandwidths.

In this paper a novel multiband planar patch antenna is presented that is based on composite right/left-handed metamaterials unit-cells. The metamaterial unit-cell employed here is implemented using L-shaped slit that is etched directly onto the radiating patch with an inductive spiral which is grounded using a via-hole. The L-shaped slit behaves as a series left-handed capacitance, and the grounded spiral act as a left-handed shunt inductance. The compact and low profile antenna exhibits desirable characteristics of wide impedance bandwidth and omnidirectional radiation in the E-plane and bi-directional in the H-plane. The antenna has dimensions of 23×17 mm^2 corresponding to $0.037\lambda_0$ by $0.027\lambda_0$ by $0.0026\lambda_0$, where λ_0 is free-space wavelength at 480 MHz. Compared to our previous work in [14]-[15], the configuration of the unit-cell in the proposed antenna results in: (1) a higher operating bandwidth; (2) predominately omnidirectional radiation pattern in the E-plane and bi-directional in the H-plane, whereas the radiation patterns of antennas in [14]-[15] are uni-directional; and (3) comparable size using a lower dielectric constant substrate.

II. DESIGN METHODOLOGY

The geometry of the proposed antenna structure, shown in Fig. 1, consists of two pairs of metamaterial unit-cells embedded in the rectangular radiating patch. Each unit-cell comprises L-shaped slit with an inductive spiral which is grounded through a metallic via-hole. The antenna is excited from left-hand side through a 50Ω microstrip feed-line. The right-hand side of the patch is terminated with a matched load of 50 ohm (SMD1206) that is connected to ground-plane through a metallic via-hole. The L-shaped slit behaves as a series left-handed capacitance, and the grounded spiral acts as a left-handed shunt inductance. The antenna is constructed on Rogers RT/ Duroid 5880 substrate with tanδ of 0.0009, dielectric constant of 2.2 and height of 1.6 mm. The physical parameters of the proposed antenna are annotated in Fig. 1 (b), where the antenna length, width and height are $L = 16$ mm, $W = 13$ mm and $h = 1.6$ mm, respectively. The antenna occupies an area of 23×17 mm^2. Other parameters are listed in Table I.

TABLE I. ANTENNA DESIGN PARAMETERS

(Lg and Wg are length and width of the ground-plane, respectively; and L_L is the length of the 1206 SMD. The dimensions are in millimeters.)

Lg	23	L	16	L_1	3.5	W_1	0.4	S_1	3.5	S_4	1.8
Wg	17	W	13	L_2	2.2	W_2	0.2	S_2	3.6	S_5	0.5
L_L	3.2	h	1.6	L_3	3	D	0.4	S_3	1.8	S_6	2.1

Standard microwave integrated circuit manufacturing technique was employed in the implementation of series left-handed (LH) capacitors (C_L) and the shunt LH inductors (L_L). The current flow over the antenna metallization results in a voltage gradient between the metallization and the ground-plane creates parasitic right-handed (RH) effects from the series inductance (L_R) and the shunt capacitance (C_R). The equivalent circuit model of the composite right/left-handed transmission-line metamaterial unit-cell, shown in Fig. 2, is therefore a combination of left-handed and right-handed transmission-line. In addition to the four reactive components (C_L, L_L, L_R and C_R) included are RH lossy components R_R and G_R, and LH lossy components G_L and R_L, which account for the dielectric loss associated with C_L and the ohmic loss associated with L_L. At low frequency, C_L and L_L are dominant, the transmission-line shows the LH characteristics; at high frequency, L_R and C_R are

dominant, the transmission-line shows the right-handed characteristics. The propagation constant, γ, of the CRLH-TL metamaterial-based antenna composed of cascaded unit-cells is given by [8]:

$$\gamma = \pm j\sqrt{(\frac{\omega}{\omega_R})^2 + (\frac{\omega_L}{\omega})^2 - K\omega_L^2} \quad (1)$$

The sign is negative in the LH frequency range, and positive in the RH range. The frequency of maximum attenuation, i.e. resonance frequency, ω_o can be derived from the roots of the derivative of the complex propagation constant in (1), thus

$$\frac{d\gamma}{d\omega} = \pm j\frac{\frac{\omega}{(\omega_R)^2} - \frac{(\omega_L)^2}{\omega^3}}{\sqrt{(\frac{\omega}{\omega_R})^2 + (\frac{\omega_L}{\omega})^2 - K\omega_L^2}} = 0 \quad (2)$$

yielding $$\omega_o = \frac{1}{\sqrt[4]{L_R C_R L_L C_L}} \quad (3)$$

The phase velocity v_p and group velocity v_g can be derived from (1), which are given by:

$$v_p = \frac{\omega}{\beta} = \pm\frac{\omega}{\sqrt{(\omega/\omega_R)^2 + (\omega_L/\omega)^2 - \kappa\omega_L^2}} \quad (4)$$

$$v_g = \frac{|\omega\,(\omega_R)^{-2} - \omega^{-3}(\omega_L)^2|}{\sqrt{\sqrt{(\frac{\omega}{\omega_R})^2 + (\frac{\omega_L}{\omega})^2 - K\omega_L^2}}} \quad (5)$$

In the purely LH case with $L_R = C_R = 0$, then from (4) and (5), $v_p = -\omega^2/\omega_L$ and $v_g = \omega^2/\omega_L$, indicating that phase velocity associated with the direction of phase propagation is negative, whereas the group velocity associated with the direction of power flow is positive. The phase and group velocities are anti-parallel. The CRLH unit-cell is engineered such that its physical size is smaller than the guided-wavelength. Under this condition the unit-cell is non-resonant. This property is exploited here to develop electrically small antenna that exhibits broad bandwidth. Current density distribution over the antenna structure at various frequencies in its operating range, shown in Fig. 3, provides further insight on the antenna. It reveals the current distribution over the antenna is more intense at 3.25 GHz.

We have modeled the series capacitances and shunt inductances using L-shaped slits and spirals, respectively, in order to minimize the antenna dimensions. However, there is no restriction on the configuration of the slits and spirals employed. Simulation analysis is necessary to determine the dimensions of the slits and spirals to enhance the antenna's impedance bandwidth and radiation characteristics. The structural parameters characterizing the antenna were optimized using 3D electromagnetic simulation tool, i.e. Ansys High Frequency Structure Simulator (HFSS). This information was then used to determine the equivalent electrical circuit model of the antenna, shown in Fig. 2, using standard parameter extraction procedures available [16], which was also verified using Keysight Technologies' ADS (RF circuit solver). The magnitudes of the optimized metamaterial unit-cell parameters are: C_L = 4.1 pF, L_L = 5.2 nH, C_R = 1.7 pF, L_R = 3.1 nH, G_L = 6.5 S, G_R = 3.8 S, R_L = 6.3 Ω and R_R = 4.9 Ω.

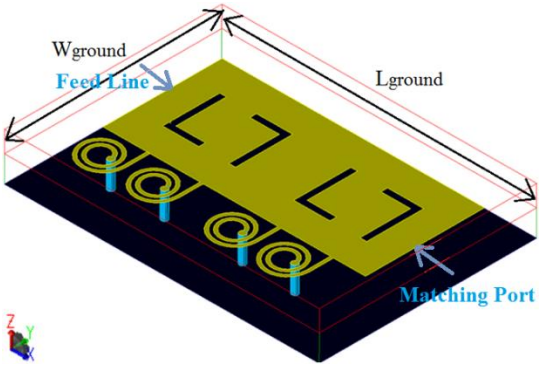

(a) Isometric view

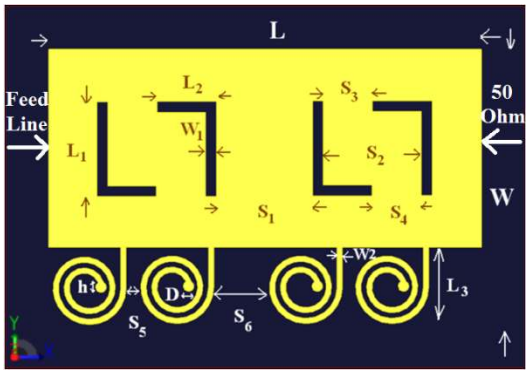

(b) Physical parameters defining the antenna configuration

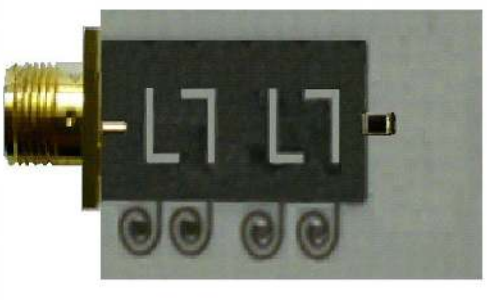

(c) Fabricated prototype

Fig. 1. Proposed metamaterial based antenna.

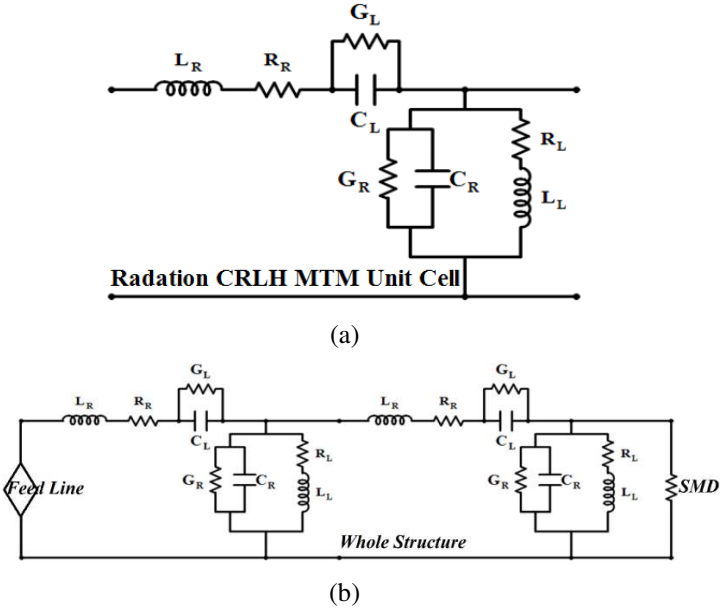

(a)

(b)

Fig. 2. Equivalent circuit model of the proposed CRLH metamaterial, a) unit-cell, and b) entire structure including feeding and matching networks.

The criteria used to determine the number of CRLH-TL unit-cells depends on a tradeoff between the antenna dimensions, impedance bandwidth and radiation characteristics. The overall goal here was to design and implement an antenna that is compact and exhibits a multi-octave impedance bandwidth with good omnidirectional radiation characteristics. The number of unit-cells was determined through optimization using High Frequency Simulator Structure (HFSS). The results in Fig. 4 show that the antenna's impedance bandwidth extends by simply increasing the number of unit-cells. In addition, the number of resonances generated correlates to the number of unit-cells. The impedance bandwidth of one unit-cell is 47.88 %, which increases to 176.97 % with four unit-cells. By cascading four metamaterial unit-cells is sufficient to provide coverage across L, S and C-bands.

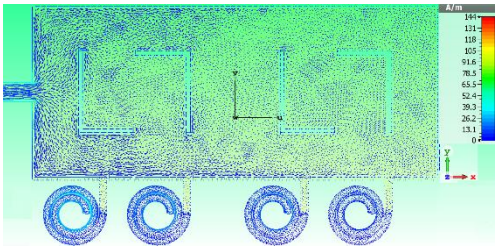

@ 400 MHz

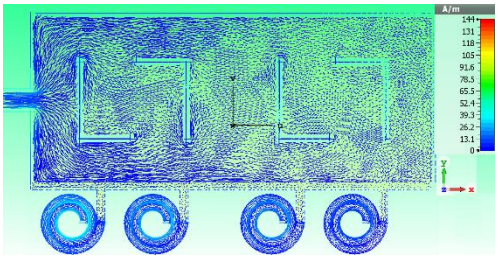

@ 3.25 GHz

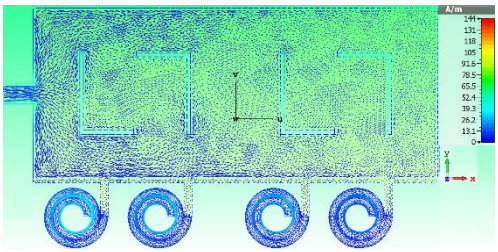

@ 6.55 GHz

Fig. 3. Current density distribution over the antenna at various frequencies in the operating range of the proposed antenna.

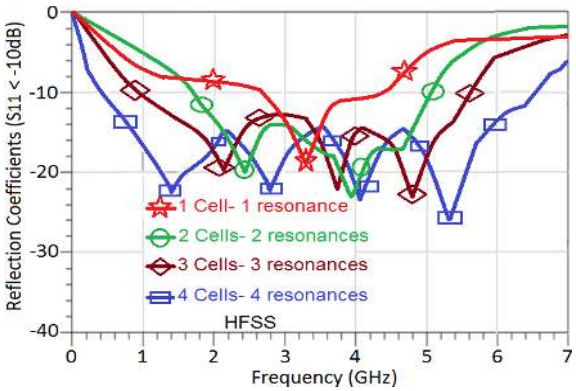

Fig. 4. Reflection coefficient response of the proposed antenna as a function of number of unit-cells.

Effect of the L-shaped slit length (L_S) and width (W_S) on the four unit-cells antenna is shown in Fig. 5. The results show a

shorter slit length and width to enhance the impedance bandwidth of the antenna. In fact, a reduction in the slit length from 4.5 mm to 3.5, and width from 0.6 mm to 0.4 mm increases the impedance bandwidth from 5.6 GHz to 6.15 GHz for reflection-coefficient better than -10 dB. The optimized length and width of the L-shaped slit were determined from these results to be 3.5 mm and 0.4 mm, respectively. The proposed antenna was constructed using four unit-cells, each of which occupying a space of 3×13 mm^2 or $0.0048\lambda_0 \times 0.021\lambda_0$, where free-space wavelength is 480 MHz. The total length and width of the antenna are $0.032\lambda_0$ (20.2 mm) and $0.021\lambda_0$ (13 mm), respectively. The antenna ground-plane occupies an area of 23×17 mm^2. The proposed antenna technique provides a low profile structure that is easy to implement using conventional MIC technology.

The measured and simulated reflection-coefficient response of the proposed antenna is shown in Fig. 6. The simulation results predict the antenna to have a bandwidth of 6.15 GHz (0.4 GHz – 6.55 GHz) for S_{11} < -10dB; however the measured bandwidth was 6.02 GHz (0.48 GHz – 6.5 GHz). The corresponding simulated and measured fractional bandwidths are 176.97 % and 172.49 %, respectively.

Besides the requirement of compact size and wide impedance bandwidth, the antenna needs to possess good radiation characteristics of gain and efficiency. The gain and efficiency performance of a typical antenna can be improved by extending its effective aperture [17]. This is conventionally achieved by simply increasing the cross-sectional area of antenna. Unfortunately, this can affect the antenna's size. Simulation results, in Fig. 7 and 8, show that the proposed antenna's effective aperture can be increased by either increasing the number of unit-cells or number of spirals or spiral turns. Antenna with four unit-cells provides a gain and efficiency of 3.68 dBi and 73.4 %, respectively, at 3.25 GHz. Increasing the spiral turns from one up to two results in marginal improvement in the gain and efficiency to 3.83 dBi and 73.7 %, respectively, at 3.25 GHz. Unlike the conventional technique the proposed technique has minimal effect on the antenna size. The simulated and measured gain and radiation efficiency for the four unit-cell antenna is shown in Fig. 9. There is good agreement between the measured and simulated results. The measured gain and efficiency are 3.7 dBi and 73 %, respectively, at 3.25 GHz.

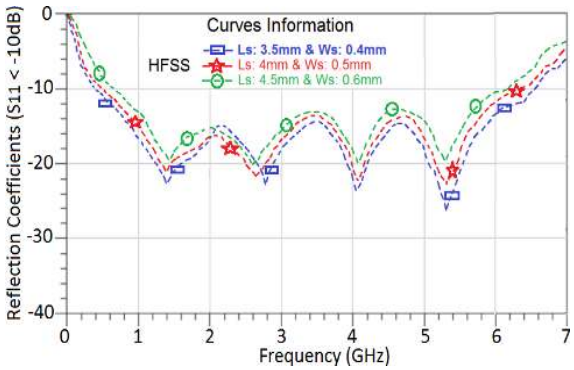

Fig. 5. Reflection-coefficient response of the proposed antenna as a function of the L-shape slit length and width. (Please note, $L_S = L_1$ and $W_S = W_1$. All other parameters in Table I were kept fixed.)

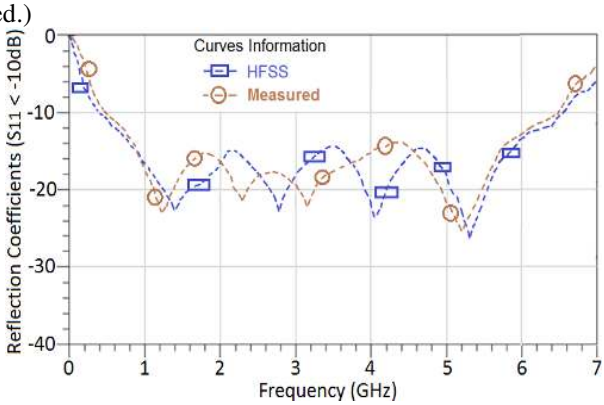

Fig. 6. Simulated and measured reflection-coefficient response of the proposed antenna.

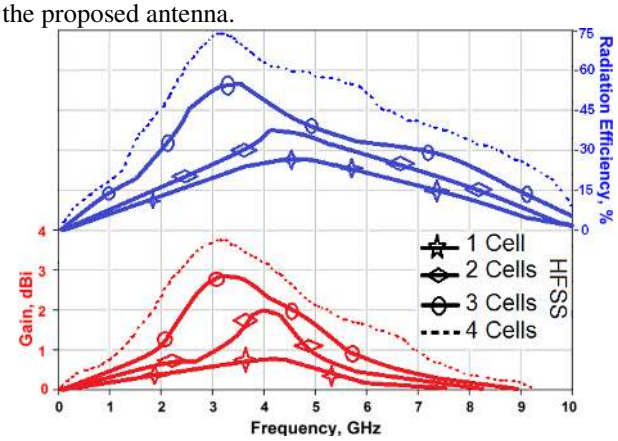

Fig. 7. Gain and efficiency performance as a function of number of unit-cells.

The simulated and measured E (*xz*)-plane and H (*yz*)-plane co- and cross-polarization radiation patterns at various spot frequencies in the antenna's operating frequency range are plotted in Figs. 10-13, respectively. The radiation is

predominately omnidirectional in the E-plane and bidirectional in the H-plane.

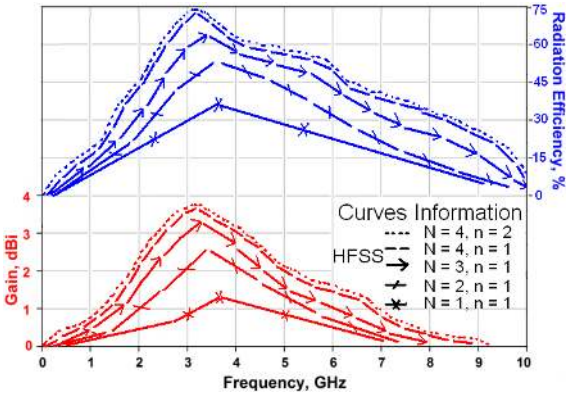

Fig. 8. Gain and efficiency performance as a function of number of spirals and spiral turns (N = number of spirals, and n = number of spiral turns).

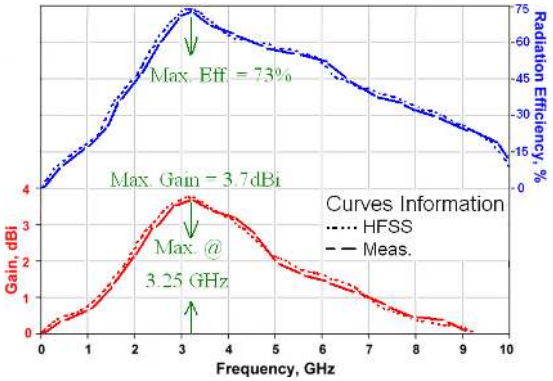

Fig. 9. Simulated and measured curves of the gain and radiation efficiency versus frequency (four unit-cells with N = 4 & n = 2).

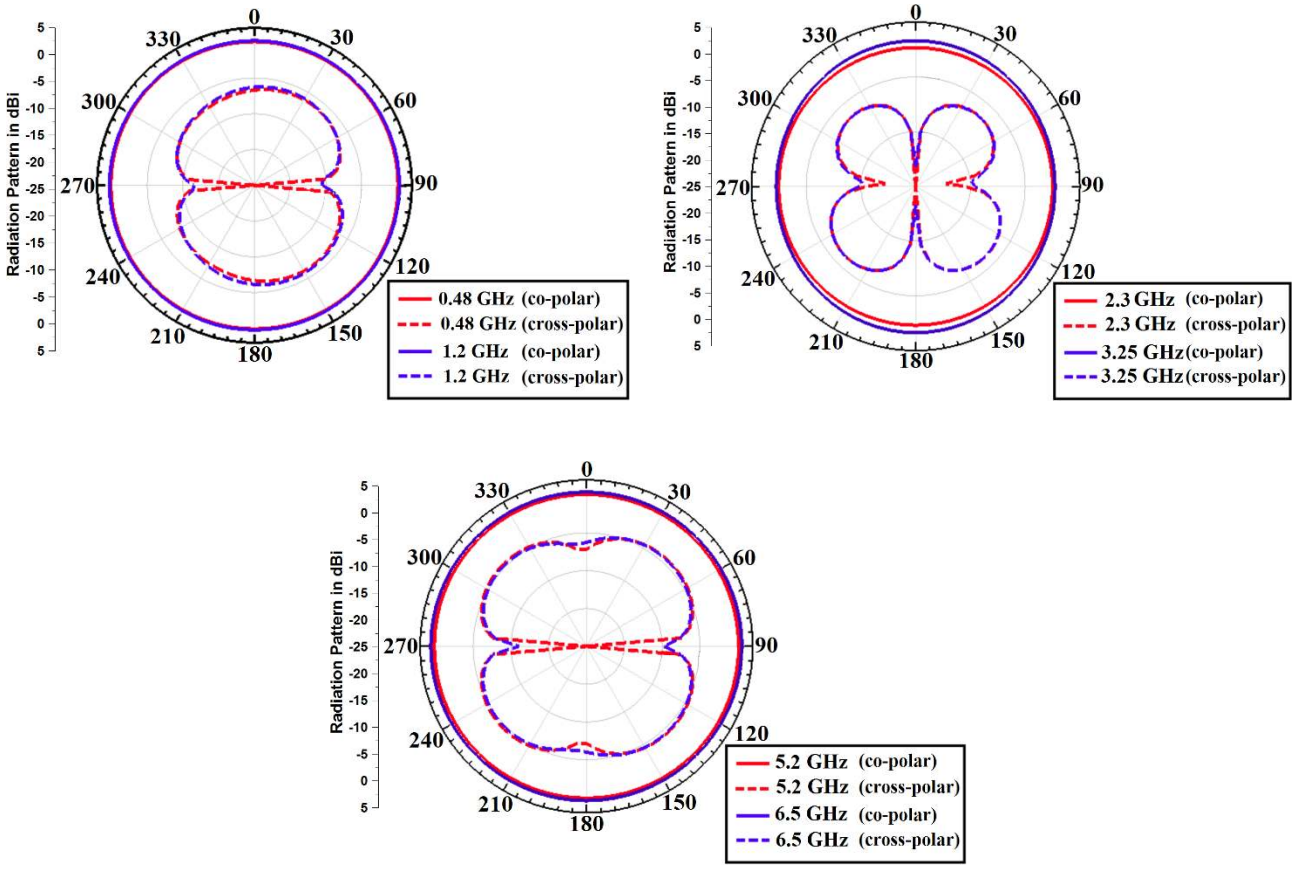

Fig. 10. Simulated E-plane co- and cross-polarization radiation patterns at various spot frequencies within the operating frequency range of the antenna.

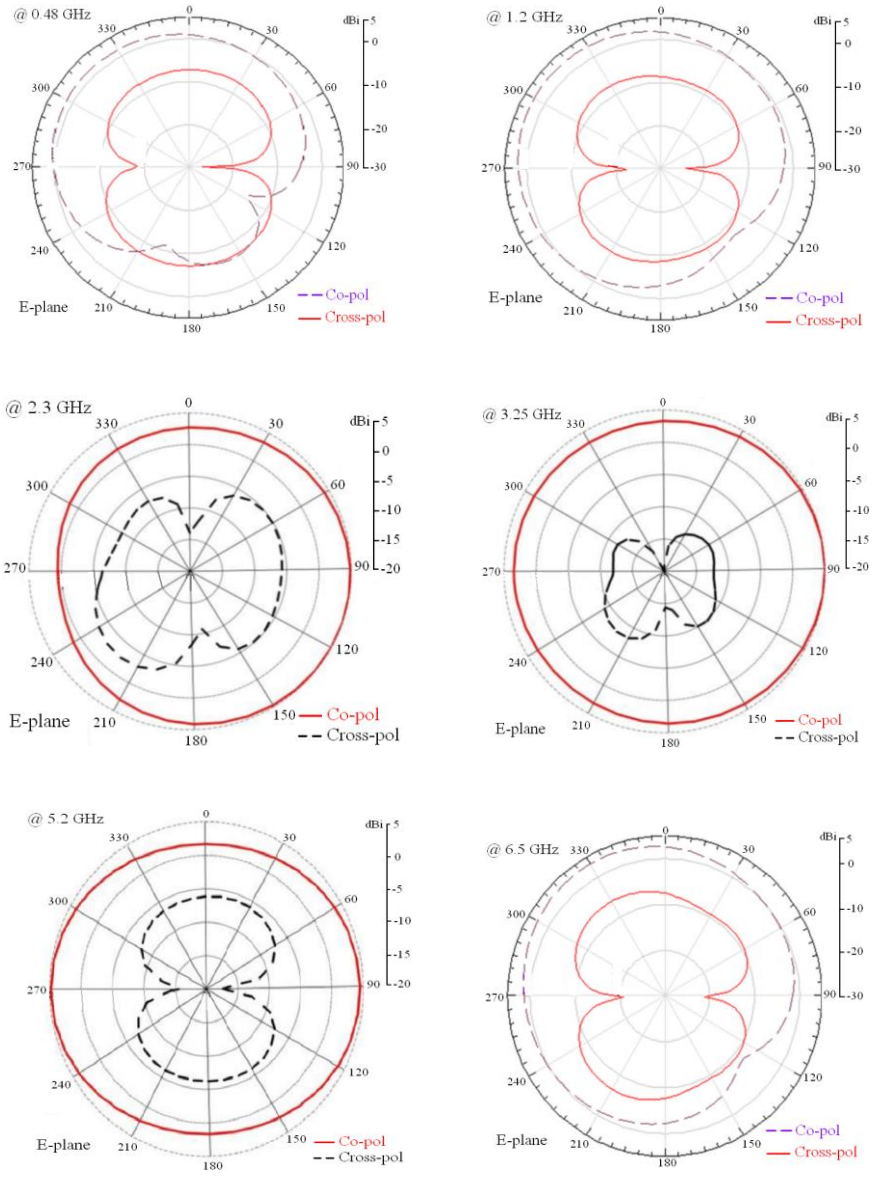

Fig. 11. Measured E-plane co- and cross-polarization radiation patterns at various spot frequencies within the operating frequency range of the antenna.

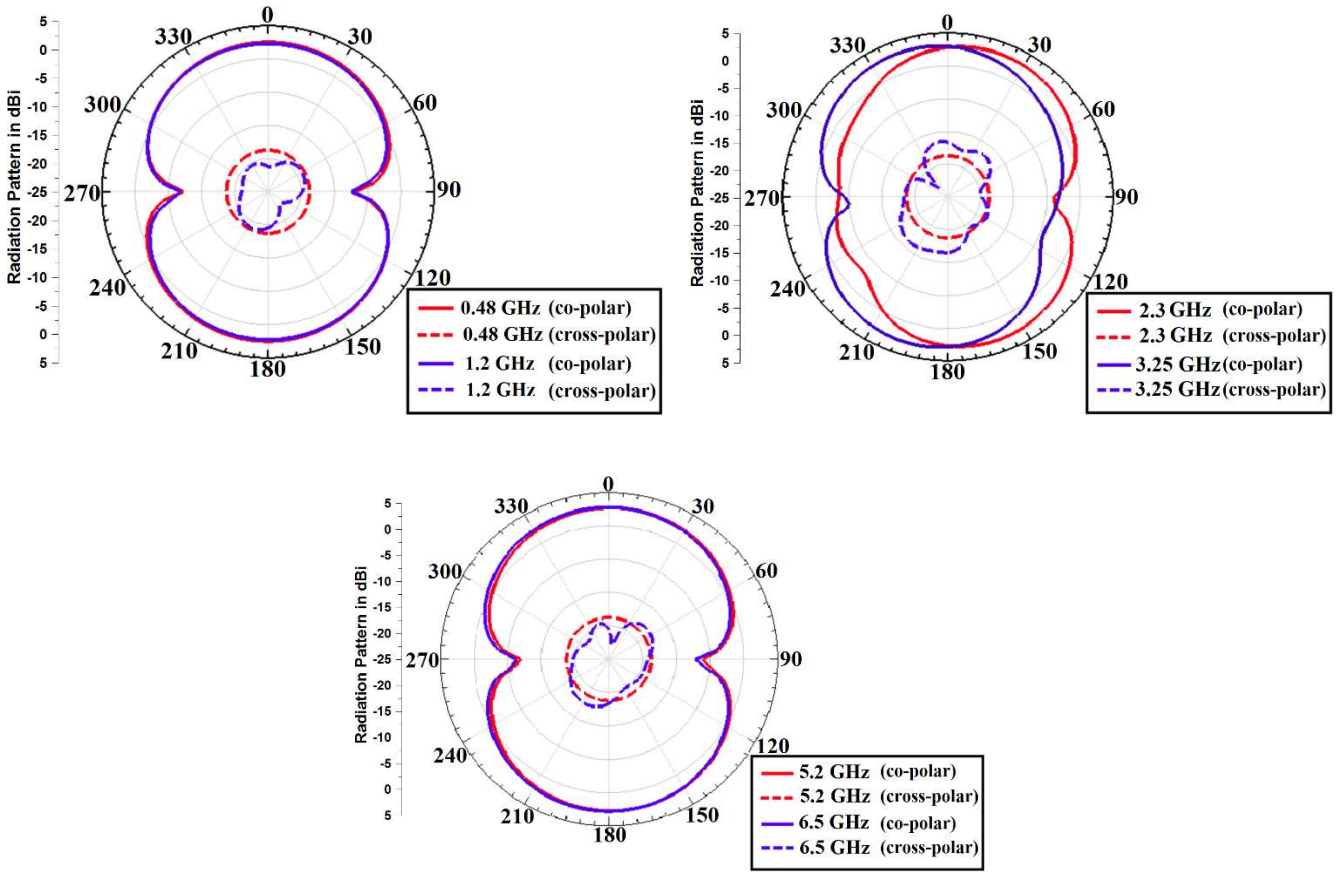

Fig. 12. Simulated H-plane co- and cross-polarization radiation patterns at various spot frequencies within the operating frequency range of the antenna.

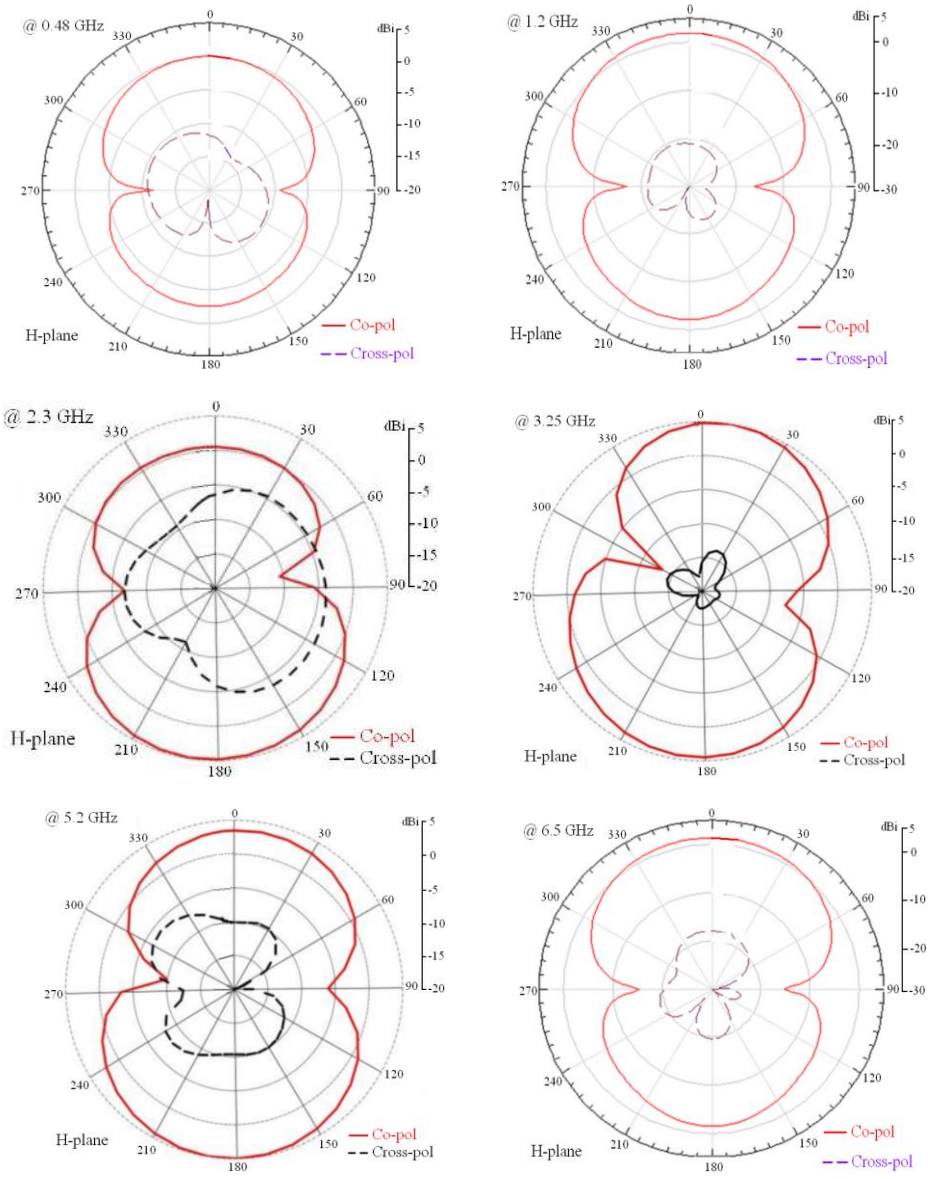

Fig. 13. Measured H-plane co- and cross-polarization radiation patterns at various spot frequencies within the operating frequency range of the antenna.

Comparison of the proposed antenna with other multiband planar antenna structures in terms of size, bandwidth, gain and efficiency performance are given in Table II. It is evident the proposed metamaterial antenna is comparable in size to existing antennas and offers in most cases a higher gain and efficiency performance. The advantage of the proposed antenna over other antennas is its exceptionally large fractional bandwidth of 172.47%.

TABLE II. SPECIFICATIONS OF THE PROPOSED ANTENNA COMPARED TO REPORTED MULTIBAND PLANAR ANTENNAS (UC represents unit-cells; FBW represents fractional bandwidth)

Papers	Dimensions	Freq. range (FBW)	Max. Gain (dBi)	Max. Eff.
[14] 2 UC antenna	(H-shape) $0.05\lambda_0\times0.023\lambda_0\times0.0027\lambda_0$ @ 1 GHz, 15×6.9×0.8 mm^3	1.2–6.7 GHz (139%)	6.8	86%
	(T-shape) $0.052\lambda_0\times0.023\lambda_0\times0.002\lambda_0$ @ 1 GHz, 15.5×6.9×0.8 mm^3	1.1–6.85 GHz (144%)	7.1	86%
[15] 6 UC antenna	$0.068\lambda_0\times0.023\lambda_0\times0.0027\lambda_0$ @ 1 GHz, 20.4×6.8×0.8 mm^3	5.8–7.3 GHz (23%)	4.8	78%
[18] 4 UC antenna	$0.047\lambda_0\times0.021\lambda_0\times0.002\lambda_0$ @ 1 GHz, 14.2×6.32×0.8 mm^3	1–3.2 GHz (104.76%)	2.3	62%
[18] 6 UC antenna	$0.064\lambda_0\times0.021\lambda_0\times0.0027\lambda_0$ @ 1 GHz, 19.2×6.32×0.8 mm^3	0.8–3.4 GHz (123.8%)	2.8	70%
[19] 8 UC antenna	$0.075\lambda_0\times0.02\lambda_0\times0.027\lambda_0$ @ 1 GHz, 22.6×7×0.8 mm^3	7.25–17.8 GHz (84.23%)	2.3	48.2%
[19] 7 UC antenna	$0.072\lambda_0\times0.02\lambda_0\times0.005\lambda_0$ @ 1 GHz, 21.7×7×1.6 mm^3	7.8–19.85 GHz (87.16%)	3.4	68.1%
[19] 6 UC antenna	$0.06\lambda_0\times0.02\lambda_0\times0.027\lambda_0$ @ 1 GHz, 18×7×0.8 mm^3	7.5–16.8 GHz (74.4%)	2.1	44.3%
[19] 5 UC antenna	$0.056\lambda_0\times0.02\lambda_0\times0.005\lambda_0$ @ 1 GHz, 16.7×7×1.6 mm^3	7.7–18.6 GHz (82.88%)	3.1	58.6%
[20]	$0.2\lambda_0\times0.05\lambda_0\times0.003\lambda_0$ @ 1 GHz, 60×16×1 mm^3	0.67–2.55 GHz (116.7%)	4.74	62.9%
[21]	$0.06\lambda_0\times0.06\lambda_0\times0.005\lambda_0$ @ 1 GHz, 18×18×1.6 mm^3	1.8–2.35 GHz (26.5%)	3.69	20%
[22]	$0.2\lambda_0\times0.017\lambda_0\times0.017\lambda_0$ @ 1 GHz, 60×5×5 mm^3	0.8–2.5 GHz (103.03%)	0.5	53.6%
[23]	$0.06\lambda_0\times0.06\lambda_0\times0.022\lambda_0$ @ 1 GHz, 18.4×18.4×6.57 mm^3	1–2 GHz (66.66%)	0.6	26%
[24]	$0.04\lambda_0\times0.04\lambda_0\times0.011\lambda_0$ @ 1 GHz, 12×12×3.33 mm^3	2.34–2.54 GHz (8.2%)	1	22%
[25]	$0.07\lambda_0\times0.08\lambda_0\times0.003\lambda_0$ @ 1 GHz, 20×25×0.8 mm^3	3.45–3.75 GHz (8.33%)	2	27%
[26]	$0.10\lambda_0\times0.09\lambda_0\times0.002\lambda_0$ @ 1 GHz, 32×28×0.8 mm^3	5.3–8.5 GHz (46.37%)	7.2	98%
[27]	$0.13\lambda_0\times0.15\lambda_0\times0.005\lambda_0$ @ 1 GHz, 40×45×1.5 mm^3	3.42–3.55 GHz (3.7%)	4.9	93%
Proposed 4 UC antenna	$0.077\lambda_0\times0.057\lambda_0\times0.005\lambda_0$ @ 1 GHz, 23×17×1.6 mm^3	0.48–6.5 GHz (172.49%)	3.7 dBi	73%

III. CONCLUSIONS

Design of a tri-band (L, S, and C-bands) antenna was presented which is based on composite right/left-handed metamaterial unit-cells. The metamaterial unit-cell is composed of L-shaped slits that are etched inside the rectangular radiating patch with a grounded inductive spiral using a metallic via-hole. The L-shaped slits essentially act as left-handed capacitance and the spiral left-handed inductance. The proposed antenna's gain and efficiency performance can be increased by simply increasing the number of unit-cells or the inductive lines spiral turns. This has minimal affect on the antenna's dimensions unlike conventional techniques that involves increasing the antenna aperture. The performance of the antennas was optimized and verified practically. The antenna operates over 0.48 GHz – 6.5 GHz and has a fractional bandwidth of 172% with a maximum gain and efficiency of 3.7 dBi and 73 %, respectively, at 3.25 GHz. The antenna radiates predominately omnidirectional in the E-plane and bi-directional in the H-plane. The electrical dimensions of the antenna are $0.037\lambda_0 \times 0.027\lambda_0 \times 0.002\lambda_0$ and $0.25\lambda_0 \times 0.18\lambda_0 \times 0.017\lambda_0$, where λ_0 is free space wavelength at 0.48 and 3.25 GHz, respectively. The antenna exhibits a superior fractional bandwidth compared to other reported multiband planar antennas. The characteristics of the antenna make it suitable for integration into portable microwave devices and use in the broadband or multiband wireless systems operating predominately across L to C-bands.

REFERENCES

[1] T. N. Chang and J. H. Jiang, "Meandered T-shaped monopole antenna," IEEE Trans. Antennas Propag., vol. 57, no. 12, pp. 3976–3978, Dec. 2009.

[2] G. Augustin, P. C. Bybi, V. P. Sarin, P. Mohanan, C. K. Aanandan, and K. Vasudevan, "A compact dual-band planar antenna for DCS-1900/ PCS/PHS, WCDMA/IMT-2000, and WLAN applications," IEEE Antennas Wireless Propag. Lett., vol. 7, pp. 108–111, 2008.

[3] W.-C. Liu and C.-F. Hsu, "Dual-band CPW-fed Y-shaped monopole antenna for PCS/WLAN application," Electron. Lett., vol. 41, pp. 390–391, 2005.

[4] B. Manimegalai, S. Raju, and V. Abhaikumar, "A multifractal cantor antenna for multiband wireless applications," IEEE Antennas Wireless Propag. Lett., vol. 8, pp. 359–362, 2009.

[5] C. P. Hsieh, T. C. Chiu, and C. H. Lai, "Compact dual-band slot antenna at the corner of the ground plane," IEEE Trans. Antennas Propag., vol. 57, no. 10, pp. 3423–3426, Oct. 2009.

[6] W. C. Liu, C. M. Wu, and N. C. Chu, "A compact CPW-fed slotted patch antenna for dual-band operation," IEEE Antennas Wireless Propag. Lett., vol. 9, pp. 595–598, 2010.

[7] K. F. Lee, S. L. S. Yang, and A. A. Kishk, "Dual- and multiband U-slot patch antennas," IEEE Antennas Wireless Propag. Lett., vol. 7, pp. 645–647, 2008.

[8] C. Caloz and T. Itoh, Electromagnetic Metamaterials, Transmission Line Theory and Microwave Applications. Wiley and IEEE Press, 2005.

[9] R. W. Ziolkowski, "An efficient, electrically small antenna designed for VHF and UHF applications" IEEE Antennas Wireless Propag. Lett., vol. 7, pp. 217–220, 2008.

[10] M. Alibakhshi-Kenari, M. Naser-Moghadasi, and R. A. Sadeghzadeh, "Composite right – left-handed-based antenna with wide applications in very-high frequency – ultra-high frequency bands for radio transceivers," IET Microwaves, Antennas & Propagation, vol. 9, issue 15, pp. 1713 – 1726, 10 Dec. 2015.

[11] M. Alibakhshi-Kenari, M. Naser-Moghadasi, R. A. Sadeghzadah, "Bandwidth and radiation specifications enhancement of monopole antennas loaded with split ring resonators," IET Microwaves, Antennas & Propagation, vol. 9, issue 14, pp. 1487 – 1496, 19 Nov. 2015.

[12] J. Zhu and G. V. Eleftheriades, "Dual-band metamaterial-inspired small monopole antenna for WiFi applications," Electron. Lett., vol. 45, no. 22, pp. 1104–1106, Oct. 2009.

[13] C.-J. Lee, K. Leong, and T. Itoh, "Composite right/left-handed transmission line based compact resonant antennas for RF module integration," IEEE Trans. Antennas Propag., vol. 54, pp. 2283–2291, Aug. 2006.

[14] M. Alibakhshi-Kenari, M.Naser-Moghadasi, R. A. Sadeghzadeh and B. S. Virdee, "Metamaterial-based Antennas for Integration in UWB Transceivers and Portable Microwave Handsets," Int. Journal of RF and Microwave Computer-Aided Engineering, vol. 26, issue 1, pp.88–96, January 2016.

[15] M. Alibakhshi-Kenari, M. Naser-Moghadasi, B. S. Virdee, A. Andújar and J. Anguera, "Compact antenna based on a composite right/left handed transmission line," Microwave and Optical Technology Letters, vol. 57, issue 8, pp. 1785–1788, August 2015.

[16] S. Otto, A. Rennings, T. Liebig, C. Caloz, K. Solbach, "An energy-based circuit parameter extraction method for CRLH leaky wave antennas," Proc. of the 4th European Conference on Antennas and Propagation, 2010, pp.1-5.
[17] C.A. Balanis, "Antenna Theory and Design," John Wiley & Sons, Hoboken, 1997.
[18] M. Alibakhshi-Kenari, "Printed planar patch antennas based on metamaterial," Electronics Letters, vol. 2, issue 1, pp. 37–42, Jan. 2014.
[19] M. Alibakhshi-Kenari "Introducing the new wideband small plate antennas with engraved voids to form new geometries based on CRLH MTM-TLs for wireless applications," Int. Journal of Microwave and Wireless Technologies, vol. 6, Issue 6, pp 629–637, Dec. 2014.
[20] J. Luo, S. Gong, P. Duan, C. Mou, and M. Long, "Small-size wideband monopole antenna with CRLH-TL for LTE mobile phone," Progress In Electromagnetics Research C, vol. 50, pp. 171–179, 2014.
[21] M. A. Abdalla, A. A. Awad, K. M. Hassan, "Wide band high selective compact metamaterial antenna for 2 GHz wireless applications," Antennas and Propagation Conf. (LAPC), pp. 350–354, Nov. 2014.
[22] Y. Li, Z. Zhang, J. Zheng and Z. Feng, "Compact heptaband reconfigurable loop antenna for mobile handset," IEEE Antennas and Wireless Propagation Letters, vol. 10, pp. 1162–1165, 2011.
[23] C. J. Lee, K. M. K. H. Leong, T. Itoh, "Composite right/left-handed transmission line based compact resonant antennas for RF module integration," IEEE Trans. Antennas Propag., vol. 54, no. 8, pp. 2283–2291, 2006.
[24] C. J. Lee, K. M. H. Leong, and T. Itoh, "Broadband small antenna for portable wireless application," Int. Workshop on Antenna Technology: Small Antennas and Novel Metamaterials, iWAT 2008, pp. 10–13, 2008.
[25] C.-C. Yu, M.-H. Huang, L.-K. Lin, Y.-T. Chang, "A compact antenna based on MTM for WiMAX," Asia-Pacific Microwave Conference, (APMC), Macau-China, Dec. 2008.
[26] Le-Wei Li, Ya-Nan Li, Tat Soon Yeo, Juan R. Mosig, and Olivier J. F. Martin, "A broadband and high-gain metamaterial microstrip antenna," Appl. Phys. Lett., 96, 164101, 2010.
[27] Tong Cai, Guang-Ming Wang, Xiao-Fei Zhang, Ya-Wei Wang, Bin-Feng Zong, He-Xiu Xu, "Compact microstrip antenna with enhanced bandwidth by loading magneto-electro-dielectric planar waveguided metamaterials," IEEE Trans. Antennas Propag., vol. 63, No.5, pp. 2306-2311, 2015.